IEEE Access
Multidisciplinary | Rapid Review | Open Access Journal

Received October 9, 2019, accepted October 21, 2019, date of publication October 28, 2019, date of current version November 8, 2019.

Digital Object Identifier 10.1109/ACCESS.2019.2949794

W-Band 8QAM Vector Millimeter-Wave Signal Generation Based on Tripling of Frequency Without Phase Pre-Coding

LUN ZHAO, LIAN XIONG, MINGXIA LIAO, JUN XIA, YUCAI PANG, AND XUEQIN SHI
Lab of Ubiquitous Wireless Communication Technology, Chongqing University of Posts and Telecommunications, Chongqing 400065, China

Corresponding author: Lun Zhao (zhaolun@cqupt.edu.cn)

This work was supported in part by the Science and Technology Research Program of Chongqing Municipal Education Commission under Grant KJ1704093, Grant KJQN201800631, and Grant KJ1600436, and in part by the Basic Theory Research and Frontier Technology Exploration Project of Chongqing under Grant cstc2018jcyjAX0302.

ABSTRACT In this paper, we propose a W-band 8-quadrature-amplitude-modulation (8QAM) frequency tripling photonic vector millimeter-wave (mm-wave) signal generation method by using a phase modulator (PM) with only amplitude pre-coding. The PM is driven by 2-Gbaud 8QAM-modulated amplitude precoded signal at 25 GHz. Instead of phase pre-coding, we only need to reverse the real part of the signal at the receiver after photo detector (PD). The structure of the transmitter and the structure of the receiver are simple. The frequency tripling scheme is completed by numerical simulation, the output optical spectrum is consistent with the theoretical analysis, and bit-error-ratio (BER) curves indicate that the put forward 75 GHz 8QAM vector signal generation technique has good performance. The BER of 6 Gbit/s 75 GHz 8QAM vector mm-wave signal is below 3.8×10^{-3} after 12 km optical fiber transmission. For all we know, it is the first time to report on the generation of high-order QAM photonic mm-wave signal with odd times of RF frequency by using a single external modulator.

INDEX TERMS Millimeter wave, frequency multiplication, phase modulation, digital signal processing, quadrature amplitude modulation.

I. INTRODUCTION

Mobile communication has developed rapidly in the past thirty years and greatly changed the people's ways of work, communication and life. In order to support the rapid development of mobile communication, a large amount of spectrum resources are required. The mm-wave band has tremendous bandwidth and can provide large capacity services. But the millimeter wave has a short transmission distance in free space because of the high propagation loss of high frequency mm-wave signal, which severely limits the application of mm-wave technique in wireless communication. Low cost and high stability photo-generated millimeter wave technology is one of the key technologies in the combination of radio over fiber (RoF) technology and mm-wave communication, which can address this issue.

In recent years, researchers have proposed some photon-based mm-wave signal generation techniques [1]–[6], such as direct modulation [7], remote optical heterodyne [8], external modulation [9]–[11], stimulated brillouin scattering (SBS) [12] and four-wave mixing (FWM) [13]. External modulation is the most widespread mm-wave signal generation scheme, which uses the two sidebands whose frequency spacing is the multiple of the radio frequency (RF) frequency to perform the frequency beating. External modulation technique can be jointed with vector modulation and digital signal processing (DSP) technique, which can not only increase spectral efficiency of the system, but also improve the sensitivity of the receiver. In addition, external modulation technique can also be jointed with optical frequency multiplication technique to produce high frequency signal generation. By choosing different two sidebands, we can get different frequency multiplication number [14]–[18].

However, in order to make the signal after photo detection and coherent demodulation is regular QPSK/QAM signal, amplitude pre-coding and/or phase pre-coding are required at the transmitter. The traditional phase pre-coding is based on phase compression to solve the phase ambiguity of

The associate editor coordinating the review of this manuscript and approving it for publication was Nianqiang Li.

the receiver. The Euclidean distance between constellation points after pre-coding is very small, which degrades the performance of the signal transmission in the system.

Aiming at this problem, we proposed a vector mm-wave signal generation method without phase pre-coding, which can realize odd times of RF frequency [19]. Since there is no phase pre-coding, the Euclidean distance between constellation points does not decrease. However, only QPSK signal is generated in our previous work and the frequency of the generated mm-wave signal is only 30GHz which is obtained by tripling of the 10GHz RF signal. 30GHz belongs to the Ka-band (28-39GHz) and considered as a candidate for satisfying 5G capacity demands [21]. Both the spectral efficiency (SE) and frequency in our previous work are low. High order QAM, such as 8QAM or 16QAM, has higher SE, and can be used in future high RoF communication.

For QPSK modulation, data is loaded on the phase, so amplitude pre-coding is unnecessary at the transmitter. While for high order QAM, data is loaded on both amplitude and phase. Thus, it is necessary to investigate whether high-order QAM vector signal generation without phase pre-coding is feasible. Moreover, W-band means the frequency of 75GHz-110 GHz, and its research is important for widening the bandwidth of RoF system. Therefore, it is necessary to investigate the generation of high-order QAM mm-wave signal without phase pre-coding at W-band.

In this paper, we propose a W-band 8QAM frequency tripling photonic mm-wave signal generation based on a single PM cascaded with a wavelength selective switch (WSS). We precode two amplitudes of 8QAM signal to suitable amplitudes so that the signal after PD is regular 8QAM constellation distribution. Phase pre-coding is not required when generating RF 8QAM signal at the transmitter. Instead, we only need to reverse the real part of the signal after PD. Since phase pre-coding is not adopting, the Euclidean distance between constellation points is large. For BTB and 12km fiber transmission schemes, the BER of 2 Gbaud 8QAM signal can reach 10^{-3} when the input optical power of PD are -12.2 dBm and -10.25 dBm, respectively. For 18km fiber transmission scheme, the BER of 2 Gbaud 8QAM signal cannot reach 3.8×10^{-3}. As far as we know, it is the first time to report on the generation of high-order QAM photonic mm-wave signal with odd times of RF frequency by using a single external modulator.

II. PRINCIPLE

Fig 1(a) shows the schematic diagram of amplitude pre-coded 8QAM mm-wave signal generation, using a frequency tripling technique enabled by a PM cascaded with a WSS. Fig. 1(b) shows the generation method of 8QAM vector RF signal without phase pre-coding. Only amplitude is precoded during the 8QAM RF vector signal generation. 8QAM RF vector signal is generated by MATLAB.

In Fig. 1(a), the continuous wave (CW) optical signal at the frequency f_c from a laser is modulated by RF carrier at the frequency f_s, which carries 8QAM data and drives the PM.

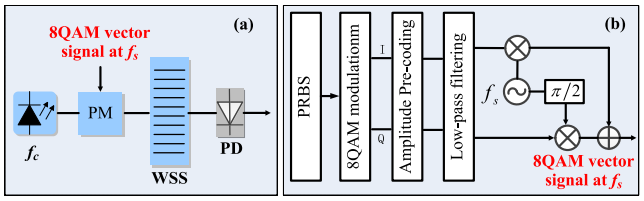

FIGURE 1. (a) Schematic diagram of photonic 8QAM signal generation at mm-wave bands based on frequency tripling technique. (b) The generation method of 8QAM vector RF signal without phase pre-coding. PRBS: Pseudo Random Binary Sequence, PM: Phase Modulator, WSS: Wavelength Selective Switch, PD: Photo Detector.

Assuming the CW optical signal at the frequency f_c can be formulated as

$$E_{CW}(t) = E_0(t)\exp(j2\pi f_c t). \tag{1}$$

where E_0 is constant and indicates the amplitude of the CW optical signal. Assuming the RF driving signal at the frequency f_s can be expressed as

$$E_{RF}(t) = V_{RF}A(t)\cos[2\pi f_s t + \varphi(t)]. \tag{2}$$

where $A(t)$ and $\phi(t)$ denote the amplitude and phase of the driving RF signal at the frequency f_s, respectively. V_{RF} is the deriving RF voltage on the PM. $A(t)$ have two values for 8QAM modulation. Thus, the output signal from the PM can be expressed as

$$\begin{aligned} E_{PM}(t) &= E_0 \exp\left\{j\pi V_{RF}A(t)\cos[2\pi f_s t + \varphi(t)]/V_\pi\right\} \\ &\quad + E_0 \exp j2\pi f_c t \\ &= E_0 \sum_{n=-\infty}^{\infty} j^n J_n(\kappa)\exp[j2\pi(f_c + nf_s)t + jn\varphi(t)]. \end{aligned} \tag{3}$$

where J_n is the first kind and order n Bessel function, V_π is half-wave voltage of the PM, and $\kappa = \pi V_{RF}A(t)/V_\pi$. The output of PM includes a central optical carrier and a series of optical sidebands. The WSS can select the desired sidebands. If we select n_1-th sideband and n_2-th sideband, the output of WSS can be formulated as

$$\begin{aligned} E_{WSS}(t) &= E_0\{j^{n_1}J_{n_1}(\kappa)\exp[j2\pi(f_c + n_1 f_s)t + jn_1\varphi(t)] \\ &\quad + j^{n_2}J_{n_2}(\kappa)\exp[j2\pi(f_c + n_2 f_s)t + jn_2\varphi(t)]\}. \end{aligned} \tag{4}$$

Then the photonic vector mm-wave signal is converted into mm-wave electrical signal by PD. The output electrical signal of the PD after isolating direct current can be formulated as

$$i_{PD}(t) = \frac{1}{2}RJ_{n_1}(\kappa)J_{n_2}(\kappa)\cos[2\pi \cdot Nf_s t + N\varphi(t)]. \tag{5}$$

where $N = n_1 - n_2$ and R indicates PD sensitivity. n_1 and n_2 represent the two sidebands choosed by WSS. It can be seen from Eq. (5) that the frequency and phase of electrical signal is N times that of the RF driving signal. If N is even, we can get the even multiple of frequency of the RF signal, and phases are indistinguishable after PD, or else we can get the odd multiple of frequency of the RF signal, and phases can be distinguished after PD for QPSK, 8QAM and 16QAM. For QPSK modulation, data is loaded on the phase of the

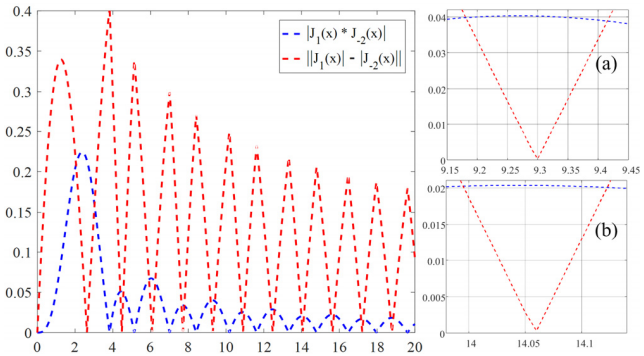

FIGURE 2. The difference and product of Bessel functions of the first kind. (a) x varies from 9.15 to 9.45. (b) x varies from 13.98 to 14.14.

signal, all we need to do is set the appropriate κ to make $|Jn_1(\kappa)|$ and $|Jn_2(\kappa)|$ equal. For high-order modulation, such as 8QAM, we also need to ensure that the amplitude of signal at the receiver meets the 8QAM distribution.

Researchers have experimentally demonstrated that the generated mm-wave vector signal based on the first-order (1st) sideband and minus second-order (−2nd) sideband, which is the same to that based on second-order (2nd) sideband and minus first -order (−1st) sideband, has a better BER performance [15]. Supposing that we choose the 1st sideband and minus −2nd sideband. Fig. 2 indicates the difference and product of Bessel functions of the first kind. The blue dotted line shows the absolute value of the product of $J_1(x)$ and $J_{-2}(x)$. The red dotted line shows the absolute value of the difference between $|J_1(x)|$ and $|J_{-2}(x)|$. Figure 2(a) is part of figure 2 when x varies from 9.15 to 9.45, the blue dotted line is 0.04 and the red dotted line is 0 when x is 9.3. It means that $|J_1(x)| = |J_{-2}(x)|$ and $J_1(x)^* J_{-2}(x) = 0.04$. Figure 2(b) is part of figure 2 when x varies from 13.98 to 14.14. It can be seen from the figure that $|J_1(x)| = |J_{-2}(x)|$ and $J_1(x)^* J_{-2}(x) = -0.02$ when x is 14.06. Therefore, the constellation of the signal after PD is still regular 8QAM distribution. Further, the constellation points with larger amplitude after amplitude pre-coding will have smaller amplitude after PD. Correspondingly, constellation points with smaller amplitude after amplitude pre-coding will have larger amplitude after PD.

Fig. 3 is the constellations distribution of 8QAM signal. Fig. 3(a) is the constellation distribution after 8QAM modulation at the transmitter. The phases corresponding to ①, ②, ③ and ④ are $\pi/4$, $3\pi/4$, $5\pi/4$, and $7\pi/4$, respectively. While the phases corresponding to ⑤, ⑥, ⑦ and ⑧ are $\pi/2$, π, $3\pi/2$, and 0, respectively. Fig. 3(b) is the constellation distribution after amplitude pre-coding.

We precoded ①, ②, ③ and ④ to smaller amplitude values, and ⑤, ⑥, ⑦ and ⑧ are precoded to larger amplitude values. $J_1(14.06)^* J_{-2}(14.06) = -0.02 < 0$, this causes ⑤, ⑥, ⑦ and ⑧ to have an additional π phase rotation after tripling of the phase. Fig. 3(c) is the constellation distribution after PD. Fig. 3(d) is the constellation distribution after reverse the real part at the receiver. Fig. 3(d) is the same as Fig. 3(a).

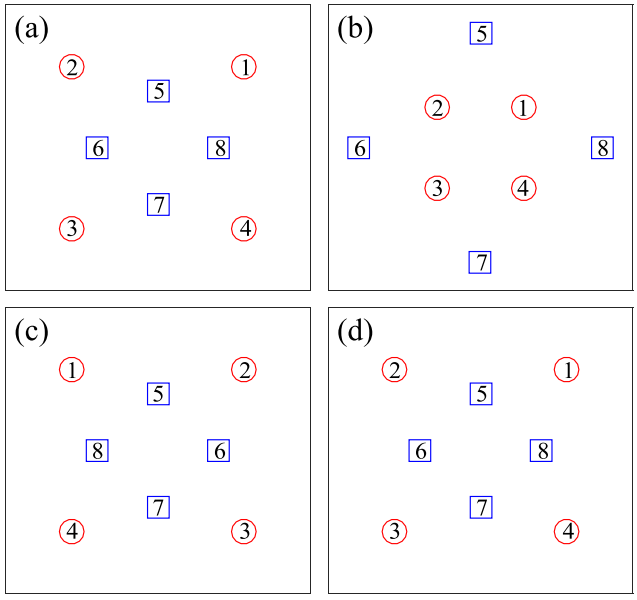

FIGURE 3. 8QAM constellations distribution. (a) After 8QAM modulation. (b) After amplitude pre-coding. (c) After PD. (d) After reverse the real part.

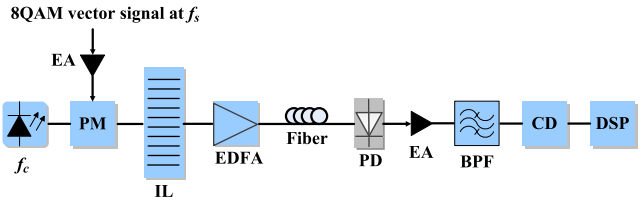

FIGURE 4. Simulation setup of the system.PM: Phase Modulator, EA: Electrical Amplifier, IL: Interleaver, EDFA: Erbium Doped Fiber Amplifier, PD: Photo Detector, BPF: Band Pass Filter, CD: Coherent Demodulation, DSP: Digital Signal Processing.

Therefore, the original signal constellation can be recovered by reverse the real part after PD at the receiver.

III. SIMULATION SETUP AND RESULTS

As shown in Fig. 4, we establish the system simulation platform and investigate the generation of 8QAM vector mm-wave signal adopting photonic frequency tripling scheme. The CW optical signal with central frequency 193.1 THz from an external cavity laser (ECL), is modulated by a 2/4 Gbaud 8QAM vector modulated signal at 25 GHz via a PM with 4V half-wave voltage. As shown in Fig. 5(a), the line width of ECL is less than 100 kHz, and the average output power of ECL is about 13 dBm. The RF signal which carrying 8QAM vector modulated data is generated in MATLAB. The pseudo-random binary sequence (PRBS) with the word length of 2^{15}-1 performs 8QAM modulation, amplitude pre-coding, low-pass filtering and up-converted into RF signal. In order to make that two sidebands choosed by interleaver (IL) or WSS roughly equal in amplitude. For frequency tripling scheme, we need to amplify the two amplitude values of the 8QAM vector modulated signal so that the corresponding modulation indexes are 9.3 and 14.06, respectively. Therefore the amplitudes of 8QAM RF signal

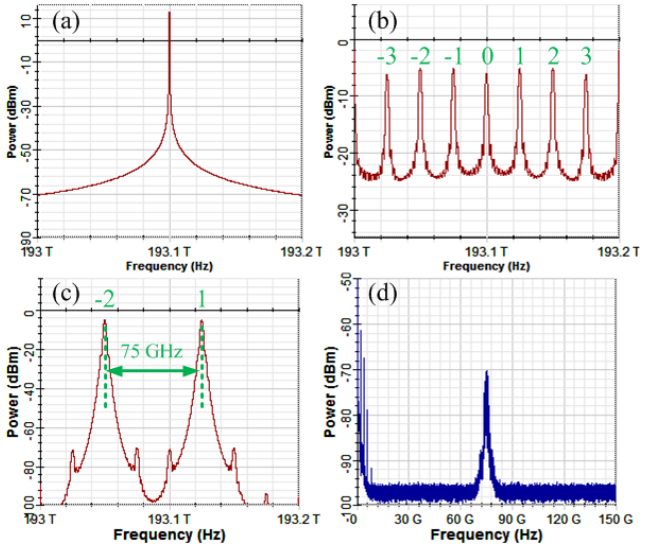

FIGURE 5. (a) Output optical spectra of ECL (0.01 nm resolution). (b) Output optical spectra of PM (0.01 nm resolution). (c) Output optical spectra of IL (0.01 nm resolution). (d) Output RF spectra of PD.

need amplify to 11.841V and 17.902V according to $\kappa = \pi V_{RF} V_0 / V_\pi$. The output optical spectrum of PM is shown in Fig. 5(b), it consists of optical carrier and a series of optical sidebands, the frequency interval is 25 GHz. The amplitude difference between the optical carrier and the sidebands are not significant. The −2nd and 1st sidebands are choosed by IL with frequency interval of 37.5 GHz and bandwidth of 5 GHz. The output optical spectrum of IL is shown in Fig. 5(c), two choosed optical sidebands have a frequency interval of 75 GHz. The side lobe suppression ratio is larger than 50 dB.

After being amplified by an Erbium-doped fiber amplifier (EDFA), the optical vector mm-wave signal is injected into single-mode fiber (SMF) -28 with attention coefficient of 0.2 dB/km, chromatic dispersion of 16.75 ps/km/nm at 1550 nm, dispersion slope of 0.075 ps/km/nm^2, and polarization mode dispersion coefficient of 0.5 ps/km$^{1/2}$.

At the receiver, the optical vector mm-wave signal is detected by a PD with the sensitivity of 1 A/W. Fig 5(d) is the RF spectrum of W-band vector mm-wave signal after PD for frequency tripling scheme when there is no fiber transmission in the system and the input optical power into PD is -9 dBm. We can see that the 75 GHz 8QAM mm-wave vector signal is dominant, while there are basically no harmonic components. This is due to the large sidelobe suppression ratio in Fig 5(c). Then we reverse the real part of the baseband signal. After that, the electrical vector mm-wave signal passes through a RF amplifier with 30 dB gain and Bessel BPF with 75 GHz central frequency and 0.9× baud rate bandwidth in turn, and then coherent demodulation by a 75 GHz local oscillator signal. In the end the binary sequence can be recovered after DSP [20], including frequency down conversion, chromatic dispersion compensation, cascaded multi-modulus algorithm (CMMA), frequency offset estimation (FOE), carrier phase estimation (CPE), and BER calculation.

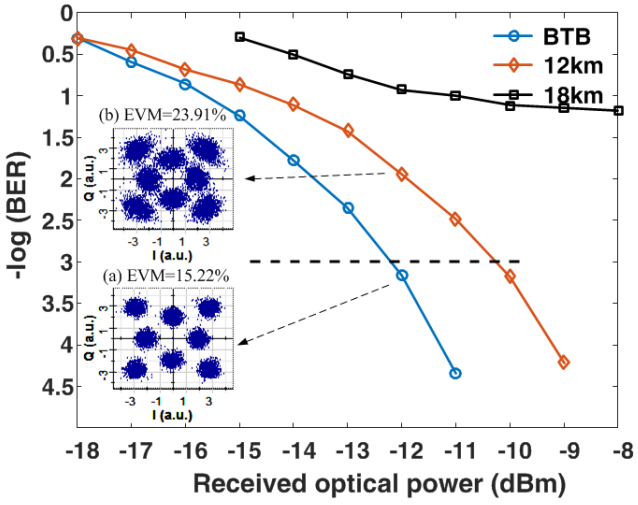

FIGURE 6. BER versus the input optical power into PD for 2 Gbaud 75 GHz 8QAM mm-wave signal.

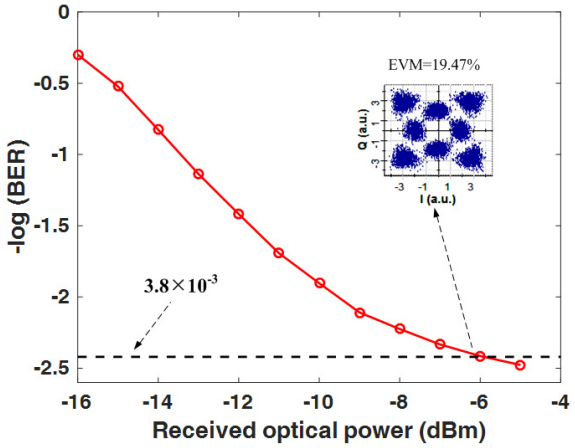

FIGURE 7. BER versus the input optical power into PD for 4 Gbaud 75 GHz 8QAM mm-wave signal.

Fig. 6 shows the BER versus the received optical power into PD for 2 Gbaud 75 GHz 8QAM vector mm-wave signal. It can be seen that 12 km SMF transmission causes about 2 dB power penalty with the BER of 10^{-3}. The insets in Fig. 6 show the constellations diagrams of 75 GHz vector mm-wave signal after offline DSP when the input optical power into PD is −12 dBm. The constellation distribution of BTB case is clearer than the constellation distribution of 12 km single-mode fiber transmission case. It is due to the dispersion effect of the single-mode fiber.

For 18km fiber transmission schemes, the BER of 2 Gbaud 8QAM signal cannot reach 3.8×10^{-3}. According to [22], we can know that 2 Gbaud 75 GHz mm-wave signal can have 24 km SMF-28 transmission distance. However, there is a gap between the transmission distance in our paper and the value of 24 km. We think that the transmission distance reduction is mainly due to insufficient bandwidth of the IL and low IL output power. The output optical power of IL is only 0.097 dBm.

Fig. 7 shows the BER versus the received optical power into PD for 4 Gbaud 75 GHz 8QAM vector mm-wave signal. For the case of BTB, the BER of 4 Gbaud 8QAM signal can reach 3.8×10^{-3}. We can see that the performance of the 4Gbaud signal is worse than the 2Gbaud in Figure 6. The insets in Fig. 7 show the constellations diagrams of 75 GHz vector mm-wave signal after offline DSP when the input optical power into PD is −6 dBm.

IV. CONCLUSION

We propose a W-band 8QAM photonic mm-wave signal generation method with three times of frequency. Only amplitude pre-coding is required in the generation of 8QAM RF signal. Instead of phase pre-coding, we only need to reverse the real part of the signal after PD. We have generated 75 GHz 8QAM mm-wave signal at 2 Gbaud by using a single PM and a WSS with frequency tripling by simulation. The simulation results show that the BER can reach the forward-error-correction (FEC) threshold 3.8×10^{-3}. The proposed frequency tripling photonic mm-wave signal generation scheme has the similar structure to the existing photonic mm-wave signal generation schemes. Therefore, the proposed scheme has good versatility.

REFERENCES

[1] J. Yu, Z. Jia, L. Yi, Y. Su, G.-K. Chang, and T. Wang, "Optical millimeter-wave generation or up-conversion using external modulators," *IEEE Photon. Technol. Lett.*, vol. 18, no. 1, pp. 265–267, Jan. 1, 2006.

[2] X. Li, J. Xiao, and J. Yu, "Long-distance wireless mm-wave signal delivery at W-band," *J. Lightw. Technol.*, vol. 34, no. 2, pp. 661–668, Jan. 15, 2016.

[3] F. Li, Z. Cao, X. Li, Z. Dong, and L. Chen, "Fiber-wireless transmission system of PDM-MIMO-OFDM at 100 GHz frequency," *J. Lightw. Technol.*, vol. 31, no. 14, pp. 2394–2399, Jul. 15, 2013.

[4] D. Zibar, R. Sambaraju, A. Caballero, J. Herrera, U. Westergren, A. Walber, J. B. Jensen, J. Martí, and I. T. Monroy, "High-capacity wireless signal generation and demodulation in 75- to 110-GHz band employing all-optical OFDM," *IEEE Photon. Technol. Lett.*, vol. 23, no. 12, pp. 810–812, Jun. 15, 2011.

[5] J. Yu, "Photonics-assisted millimeter-wave wireless communication," *IEEE J. Quantum Electron.*, vol. 53, no. 6, Dec. 2017, Art. no. 8000517.

[6] K. Kitayama, A. Maruta, and Y. Yoshida, "Digital coherent technology for optical fiber and radio-over-fiber transmission systems," *J. Lightw. Technol.*, vol. 32, no. 20, pp. 3411–3420, Oct. 15, 2014.

[7] W. Li and J. Yao, "Microwave generation based on optical domain microwave frequency octupling," *IEEE Photon. Technol. Lett.*, vol. 22, no. 1, pp. 24–26, Jan. 2010.

[8] J. Yu, X. Li, and N. Chi, "Faster than fiber: Over 100-Gb/s signal delivery in fiber wireless integration system," *Opt. Express*, vol. 21, no. 19, pp. 22885–22904, Sep. 2013.

[9] J. Xiao, X. Li, Y. Xu, Z. Zhang, L. Chen, and J. Yu, "W-band OFDM photonic vector signal generation employing a single Mach-Zehnder modulator and precoding," *Opt. Express*, vol. 23, no. 18, pp. 24029–24034, Sep. 2015.

[10] X. Li, J. Zhang, J. Xiao, Z. Zhang, Y. Xu, and J. Yu, "W-band 8 QAM vector signal generation by MZM-based photonic frequency octupling," *IEEE Photon. Technol. Lett.*, vol. 27, no. 12, pp. 1257–1260, Jun. 15, 2015.

[11] X. Li, J. Xiao, and J. Yu, "W-band vector millimeter-wave signal generation based on phase modulator with photonic frequency quadrupling and precoding," *J. Lightw. Technol.*, vol. 35, no. 13, pp. 2548–2558, Jul. 1, 2017.

[12] M. Baskaran and R. Prabakaran, "Photonic generation of microwave pulses using Stimulated Brillouin Scattering (SBS)-based carrier processing and data transmission for Radio over Fiber (RoF) systems," in *Proc. IEEE Int. Conf. Wireless Commun. Signal Process. Netw. (WiSPNET)*, Chennai, India, Mar. 2016, pp. 372–375.

[13] T. Wang, H. Chen, M. Chen, J. Zhang, and S. Xie, "High-spectral-purity millimeter-wave signal optical generation," *J. Lightw. Technol.*, vol. 27, no. 12, pp. 2044–2051, Jun. 15, 2009.

[14] L. Zhao, J. Yu, L. Chen, P. Min, J. Li, and R. Wang, "16 QAM vector millimeter-wave signal generation based on phase modulator with photonic frequency doubling and precoding," *IEEE Photon. J.*, vol. 8, no. 2, Apr. 2016, Art. no. 5500708.

[15] X. Li, Y. Xu, J. Xiao, and J. Yu, "W-band millimeter-wave vector signal generation based on precoding-assisted random photonic frequency tripling scheme enabled by phase modulator," *IEEE Photon. J.*, vol. 8, no. 2, Apr. 2016, Art. no. 5500410.

[16] W. Zhou, X. Li, and J. Yu, "Pre-coding assisted generation of a frequency quadrupled optical vector D-band millimeter wave with one Mach-Zehnder modulator," *Opt. Express*, vol. 25, no. 22, pp. 26483–26491, Oct. 2017.

[17] J. Lu, Z. Dong, J. Liu, X. Zeng, Y. Hu, and J. Gao, "Generation of a frequency sextupled optical millimeter wave with a suppressed central carrier using one single-electrode modulator," *Opt. Fiber Technol.*, vol. 20, no. 5, pp. 533–536, Oct. 2014.

[18] H. Zhang, L. Cai, S. Xie, K. Zhang, X. Wu, and Z. Dong, "A novel radio-over-fiber system based on carrier suppressed frequency eightfold millimeter wave generation," *IEEE Photon. J.*, vol. 9, no. 5, Oct. 2017, Art. no. 7203506.

[19] L. Zhao, L. Xiong, M. Liao, S. Liu, and X. Yu, "QPSK vector millimeter-wave signal generation based on odd times of frequency without precoding," *IEEE Photon. J.*, vol. 10, no. 6, Dec. 2018, Art. no. 5502109.

[20] J. Yu and X. Zhou, "Ultra-high-capacity DWDM transmission system for 100G and beyond," *IEEE Commun. Mag.*, vol. 48, no. 3, pp. S56–S64, Mar. 2010.

[21] *5G/NR-FR/Operating Bandwidth*. Accessed: Aug. 14, 2019. [Online]. Available: http://www.sharetechnote.com/html/5G/5G_FR_Bandwidth.html

[22] J. Ma, J. Yu, C. Yu, X. Xin, J. Zeng, and L. Chen, "Fiber dispersion influence on transmission of the optical millimeter-waves generated using LN-MZM intensity modulation," *J. Lightw. Technol.*, vol. 25, no. 11, pp. 3244–3256, Nov. 2007.

LUN ZHAO received the M.S. degree in communication and information system from the Wuhan Research Institute (WRI), Hubei, China, in 2012, and the Ph.D. degree in electronic science and technology from the School of electronic engineering, Beijing University of Posts and Telecommunications, Beijing, China, in 2016. He is currently working in information and telecommunication engineering with the Ubiquitous Wireless Communication Technology Team, Chongqing University of Posts and Telecommunications. His research interests include radio over fiber, coherent optical communication, machine learning/deep learning in optical communication, optical physical layer security, and 5G mobile networks.

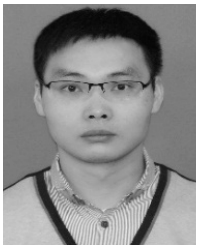

LIAN XIONG was born in Huanggang, Hubei, China, in 1985. He received the B.S. degree in telecommunications engineering from the North University of China, Taiyuan, China, in 2008, the M.S. degree in communication and information system from the Taiyuan University of Technology, Taiyuan, in 2011, and the Ph.D. degree in communication and information system from Wuhan University, Wuhan, China, in 2016. He is currently a Lecturer with the School of Communication and Information Engineering, Chongqing University of Posts and Telecommunications. His research interests include optical communication, data mining, distributed storage, and the Internet of Things.

MINGXIA LIAO received the M.Sc. degree in communication and information systems from the Chongqing University of Posts and Telecommunications, Chongqing, China, in 2010, and the Ph.D. degree in electronics science and technology from the Beijing University of Posts and Telecommunications, Beijing, China, in 2016. She is currently working in information and telecommunication engineering with the Ubiquitous Wireless Communication Technology Team, Chongqing University of Posts and Telecommunications. Her research interests include optical communication, 5G mobile networks, and mobile edge computing.

JUN XIA received the B.S. degree in computer science and the M.Eng. degree in electronics and communications engineering from the Chongqing University of Posts and Telecommunications, Chongqing, China, in 2002 and 2005, respectively. He is currently a Senior Engineer with the Chongqing University of Posts and Telecommunications. His research interests include optical communication, energy aware task scheduling on multicores/multiprocessors, 5G mobile networks, and the low-power IoT technology.

YUCAI PANG received the M.Sc. degree in communication and information systems and the Ph.D. degree in signal and information processing from Harbin Engineering University, Harbin, China, in 2012 and 2014, respectively. He is currently working in information and telecommunication engineering with the Ubiquitous Wireless Communication Technology Team, Chongqing University of Posts and Telecommunications. His research interests include array signal processing and optical communication.

XUEQIN SHI received the B.S. degree in communication engineering from the Anhui Xinhua University of Posts and Telecommunications, Hefei, China, in 2017, where she is currently pursuing the M.S. degree in information and telecommunication engineering at Chongqing University of Posts and Telecommunications.